Journal of Polymer Science Part A:
Polymer Chemistry

Energy Transfer from Fluorene Based Conjugated Polyelectrolytes to On-chain and Self-Assembled Porphyrin Units

Journal:	*J. Polym Sci. Part A: Polym. Chem.*
Manuscript ID:	JPOL-A-11-0953.R1
Wiley - Manuscript type:	Original Article
Keywords:	conjugated polymers < C, self-assembly < S, hydrophilic polymers < H, fluorescence < F, water-soluble polymers < W

Table 1.

Solvent	Absorption max (nm)	Emission max (nm)	Φ_F PF λ_{exc} 362 (nm)	Φ_FDPP λ_{exc} 362 (nm)
Dioxane Water (1:1)	365, 420 (PF, DPP)	410, 650 (PF, DPP)	0.41	0.013
1×10^{-4} M aqueous $C_{12}E_5$	367, 425 (PF, DPP)	411, 655 (PF, DPP)	0.34	0.017

Table 2.

	λ_{em} (nm)	**τ_1 (ns)**	**τ_2 (ns)**	**τ_3 (ns)**	**τ_4 (ns)**	**a_{i1}**	**a_{i2}**	**a_{i3}**	**a_{i4}**	**χ^2**
Dioxane - Water (1:1)	410	0.06	—	0.55	—	0.140	—	0.860	—	1.05
	650	—	0.13	0.61	4.87	—	0.227	0.401	0.372	0.98
$C_{12}E_5$	410	0.05	—	0.59	—	0.388	—	0.612	—	1.04
	650	—	0.37	—	4.89	—	0.366	—	0.634	0.96

Table 3.

Solvent	TPPS (M)	Φ_F PF [a] λ_{exc} 382 (nm)	Φ_F TPPS [b] λ_{exc} 382 (nm)
Dioxane Water (1:1)	2.44×10^{-6}	0.06	0.07
$C_{12}E_5$	2.44×10^{-6}	0.05	0.03

[a] reference used, quinine sulphate;

[b] reference used, TPP.

Table 4.

Solvent	System	R_0 (Å)
Dioxane Water (1:1)	PBS-PFP-DPP	62
	PBS-PFP/TPPS	47
$C_{12}E_5$	PBS-PFP-DPP	61
	PBS-PFP/TPPS	50

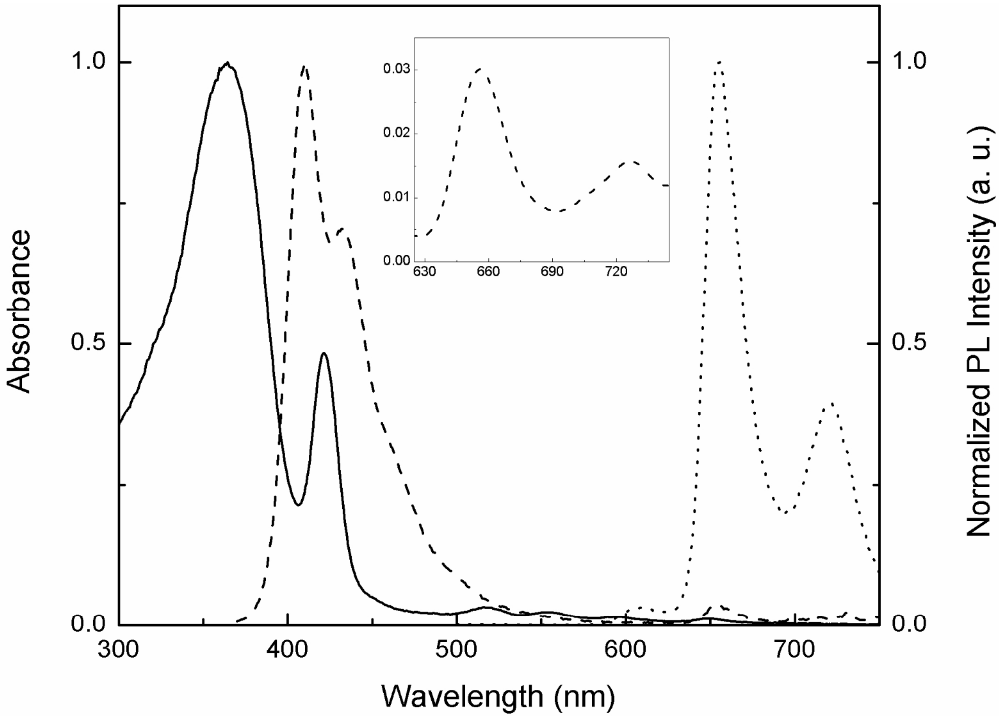

Absorption (solid line) and emission spectra (dashed line) of PBS-PFP-DPP in dioxane-water (1:1), with excitation at 365 nm (dashed line) and 420 nm (dotted line). The inset depicts the 600 – 750 nm region of the PBS-PFP-DPP emission shown in the main plot.
177x126mm (300 x 300 DPI)

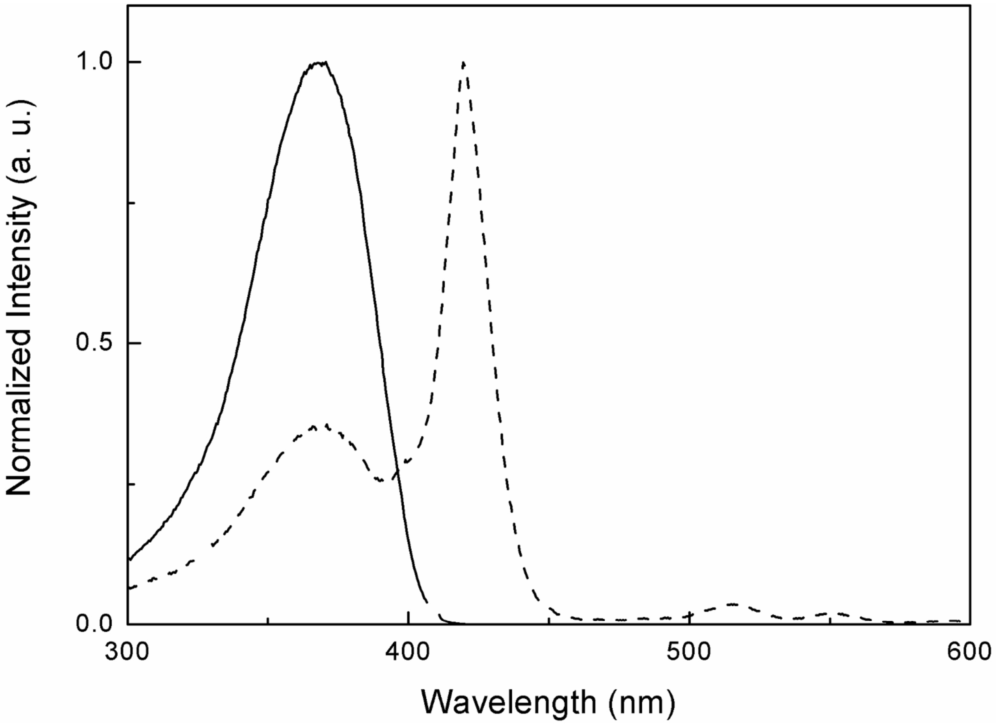

Fluorescence excitation spectra with emission at 410 nm (solid line) and emission at 655 nm (dashed line) of PBS-PFP-DPP in dioxane-water (1:1).
177x128mm (300 x 300 DPI)

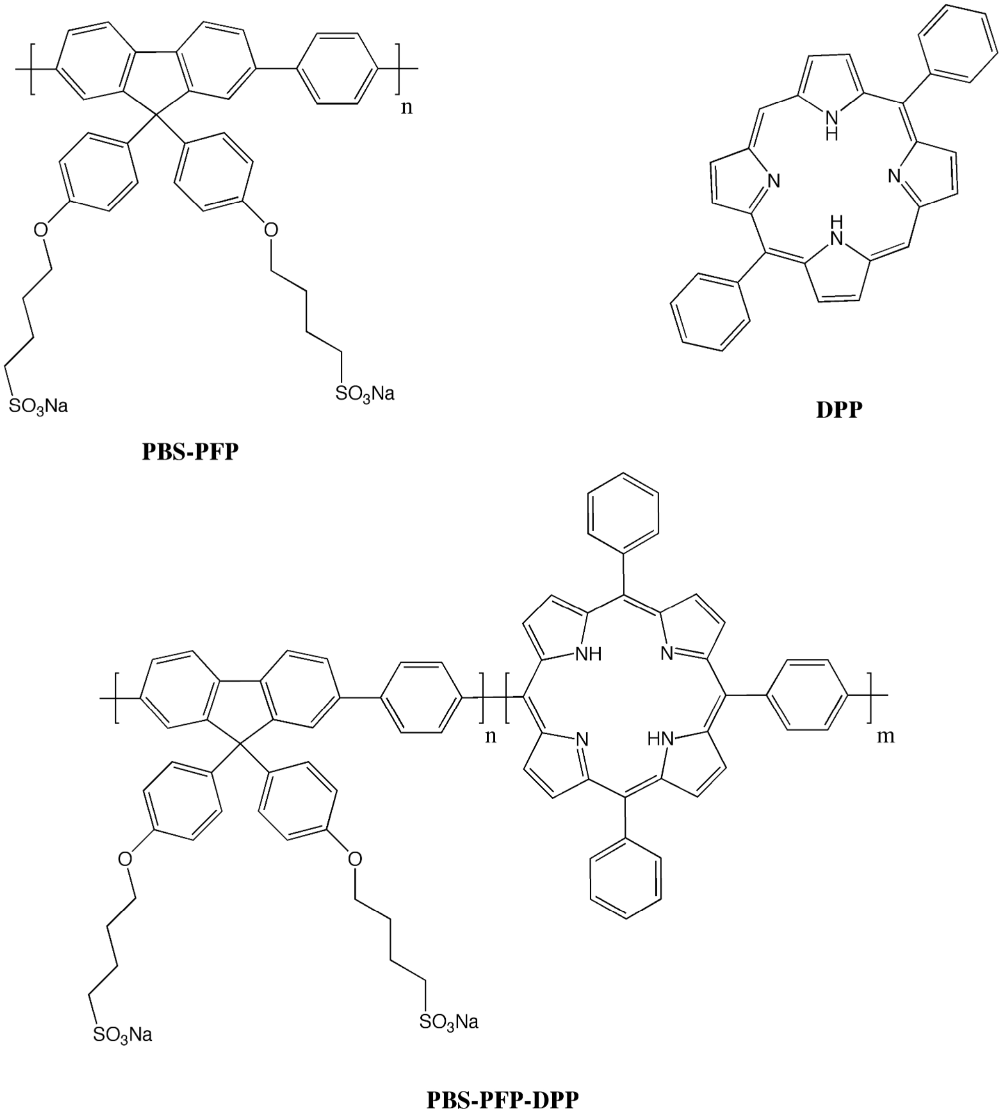

Chemical structures of the homopolymer PBS-PFP, the DPP monomer and the copolymer PBS-PFP-DPP.
260x288mm (300 x 300 DPI)

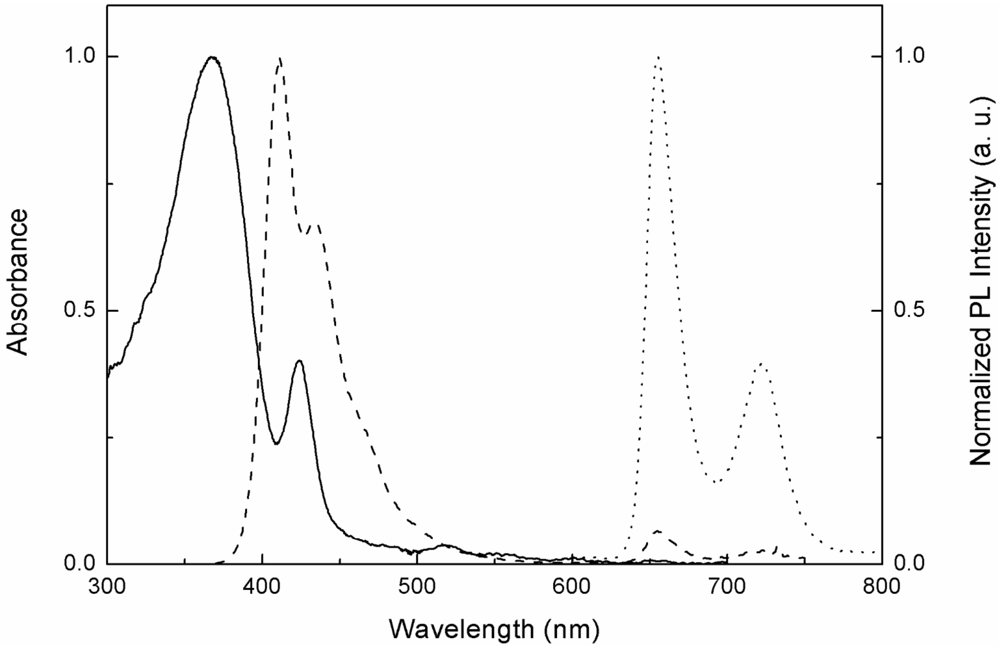

Absorption (solid line) and emission spectra (dashed line) of PBS-PFP-DPP in 1×10-4 M aqueous C12E5 solution, with excitation at 365 nm (solid line) and 420 nm (dotted line).
177x114mm (300 x 300 DPI)

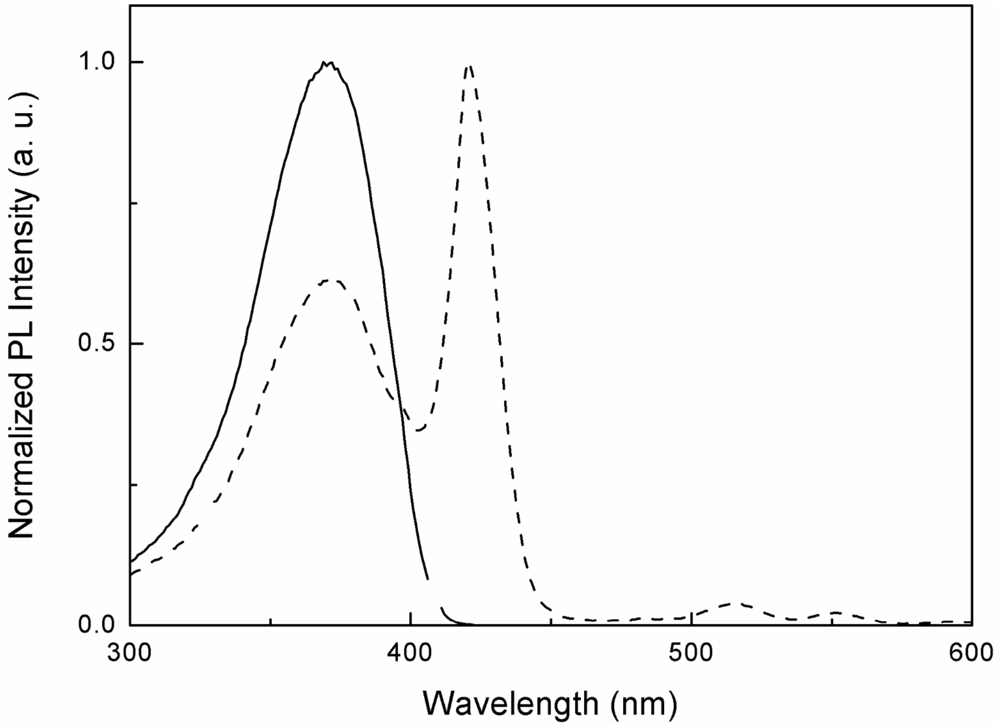

Fluorescence excitation spectra with emission at 410 nm (solid line) and emission at 655 nm (dashed line) of PBS-PFP-DPP in 1×10-4 M aqueous C12E5.
177x128mm (300 x 300 DPI)

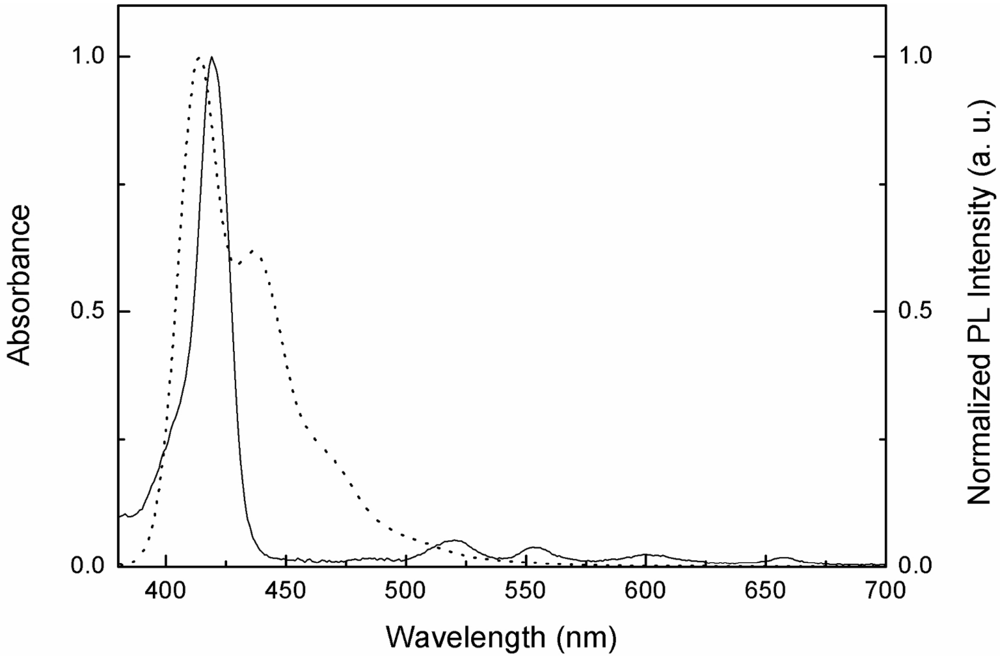

Spectral overlap between the donor PBS-PFP (dotted line) and the acceptor DPP (full line).
177x116mm (300 x 300 DPI)

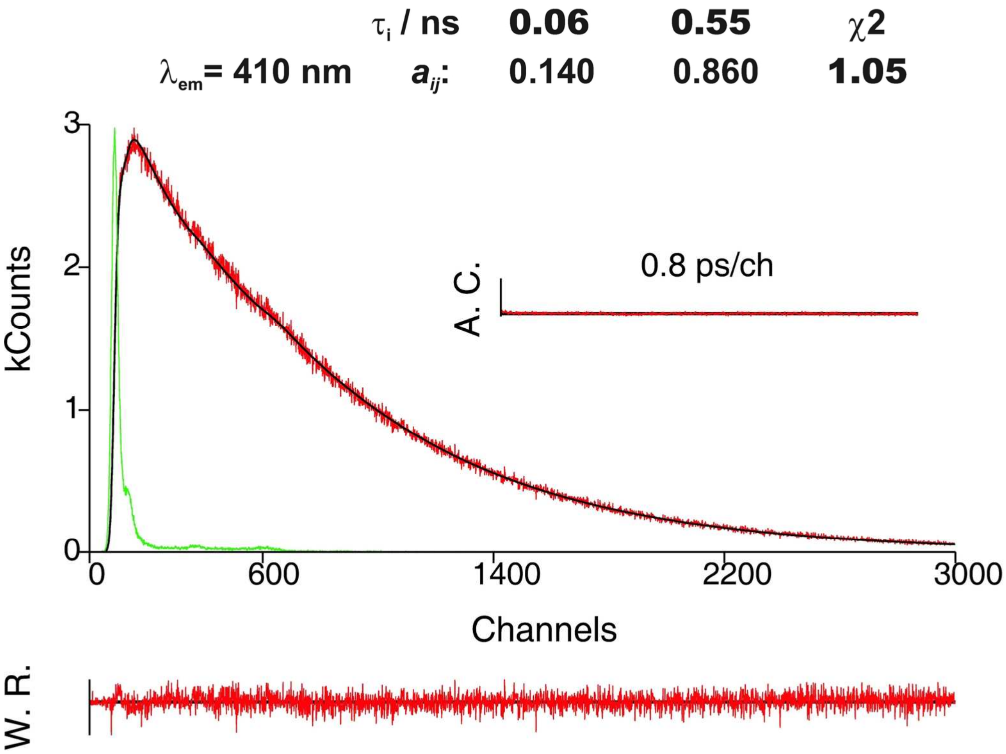

Fluorescence emission decay for PBS-PFP-DPP in dioxane water (1:1) collected at 410 nm obtained with λexc 372 nm at 298.15 K. The gray lines in the decays are the instrumental response function (IRF). For a better judgment of the quality of the fits, weighted residuals (W.R. scale, -3 ≤ σ ≤ +3), autocorrelation functions (A.C.) and χ2 are also presented.
150x112mm (300 x 300 DPI)

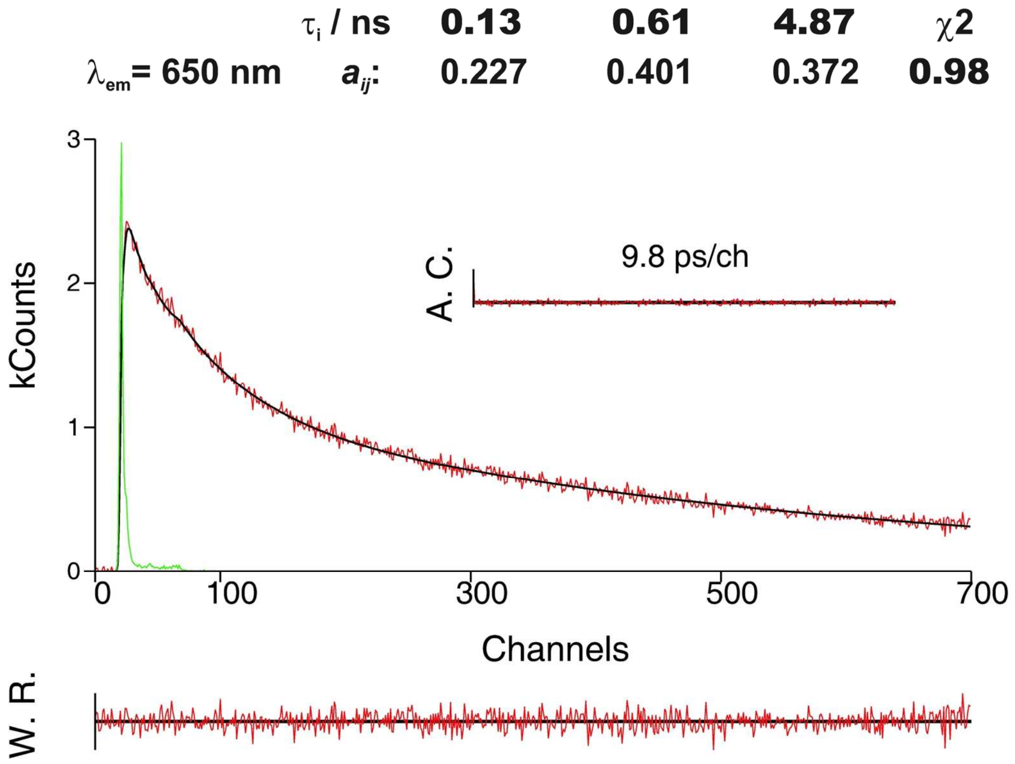

Fluorescence emission decay for PBS-PFP-DPP in dioxane water (1:1) collected at 650 nm obtained with λexc 372 nm at 298.15 K. The green lines in the decays are the instrumental response function (IRF). For a better judgment of the quality of the fits, weighted residuals (W.R. scale, -3 ≤ σ ≤ +3), autocorrelation functions (A.C.) and χ2 are also presented.
151x113mm (300 x 300 DPI)

henylporphyrinsulfonate, TPPS.
)

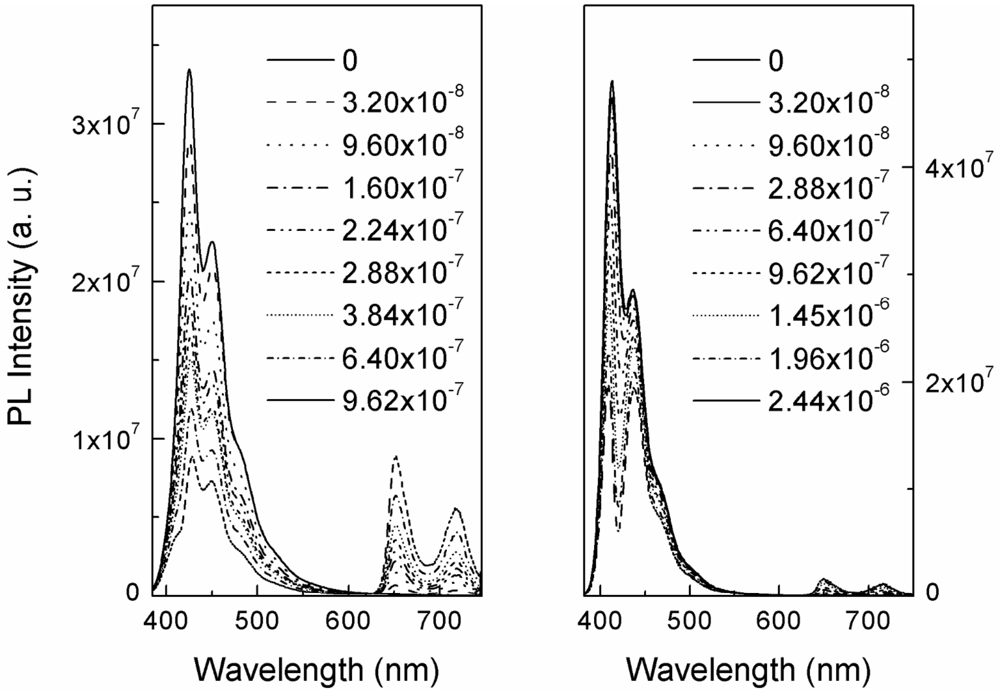

Photoluminescence spectra of PBS-PFP/Ca2+ with increasing TPPS concentrations in water dioxane (1:1) (left) and in 1×10-4M C12E5 (right). Ca2+ concentration 2x10-3 M.
177x122mm (300 x 300 DPI)

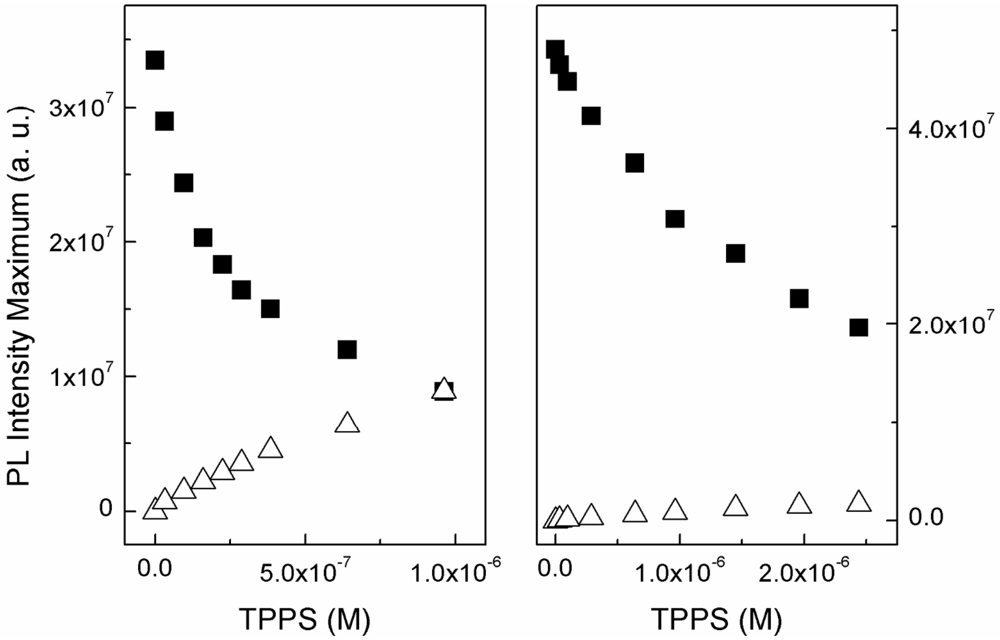

Photoluminescence maximum intensity as a function of TPPS concentration in water dioxane (1:1) (left) and in 1×10-4M C12E5 (right); squares: PBS-PFP emission and triangles: TPPS emission.
177x112mm (300 x 300 DPI)

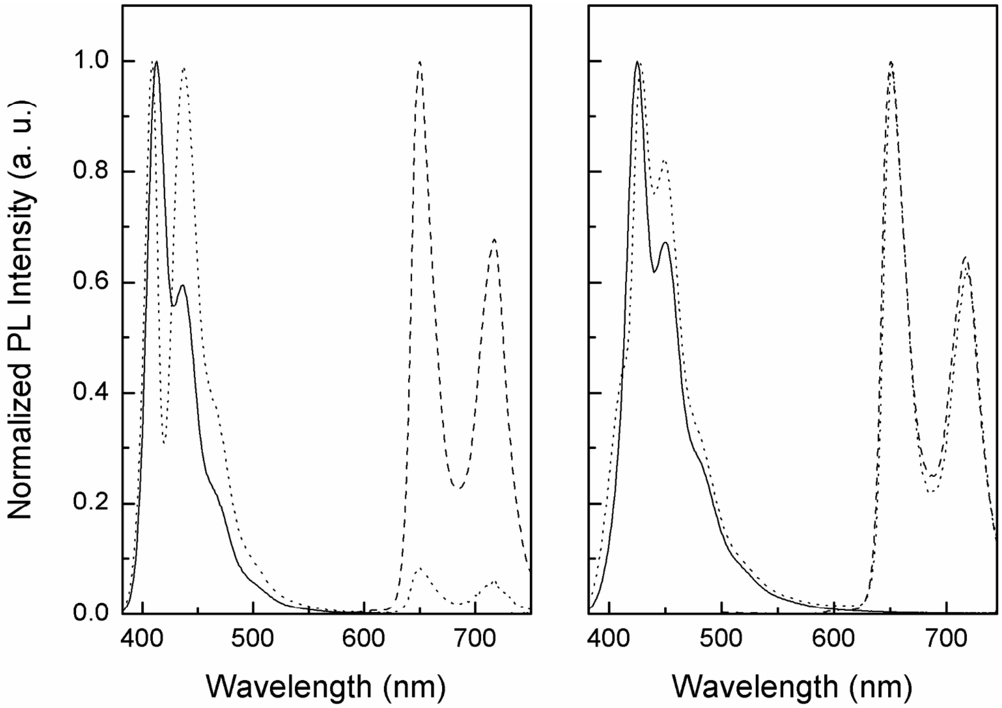

Photoluminescence spectra of PBS-PFP without TPPS (solid line) and with maxima TPPS concentration (dot line), obtained with excitation in the PF absorption maximum and TPPS emission (dash line) obtained with excitation at 420 nm, in water dioxane (1:1) (right) and in 1×10-4M C12E5 (left).
177x125mm (300 x 300 DPI)

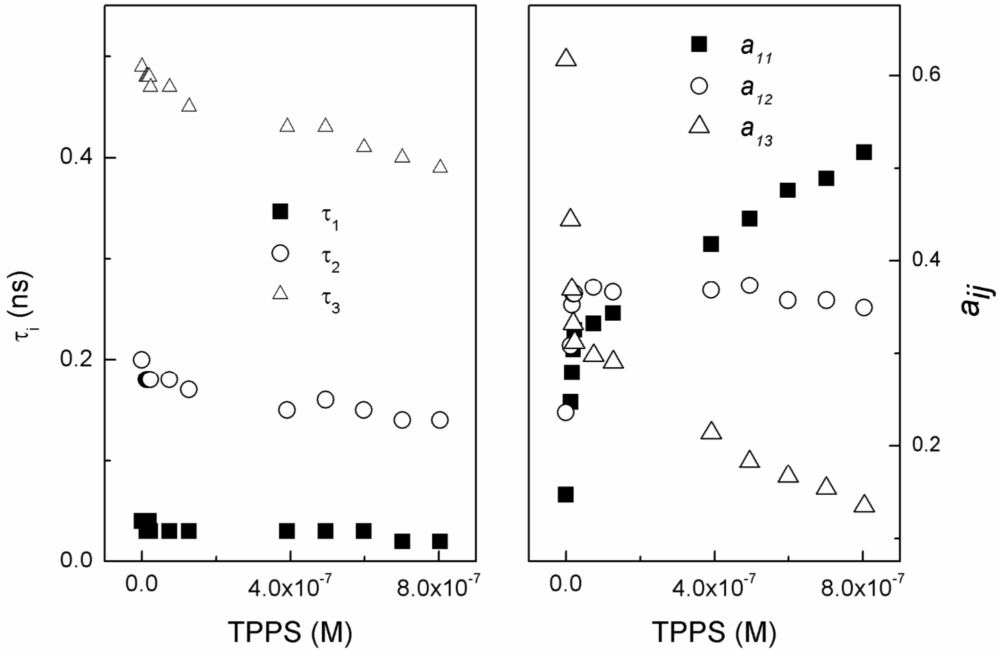

Fluorescence decay times (τi) and amplitudes (aij) of PBS-PFP (10-6 M) with Ca2+ (1×10-3 M) in 1×10-4 M C12E5 as a function of TPPS concentration.
177x115mm (300 x 300 DPI)

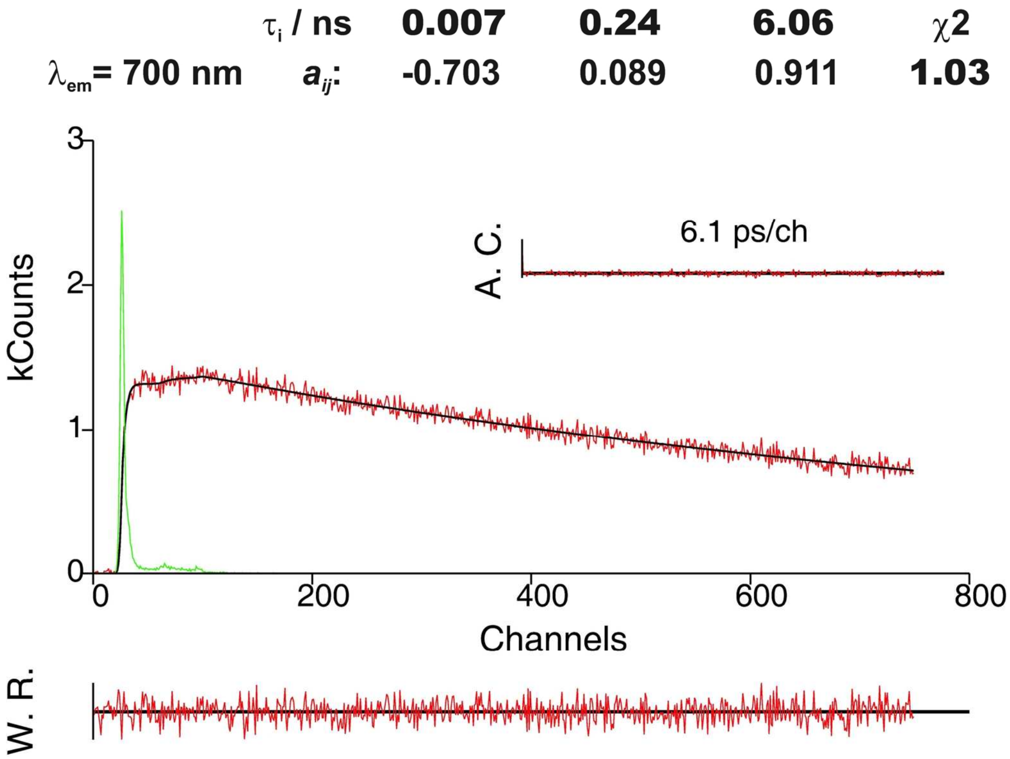

Fluorescence emission decay of PBS-PFP (10-6 M) with Ca2+ (1×10-3 M) in 1×10-4 M C12E5 and TPPS concentration maxima, obtained with λexc 392 nm at 298.15 K. The gray lines in the decays are the instrumental response function (IRF). For a better judgment of the quality of the fits weighted residuals (W.R. scale, -3 ≤ σ ≤ +3), autocorrelation functions (A.C.) and χ2 are also presented.
150x112mm (300 x 300 DPI)

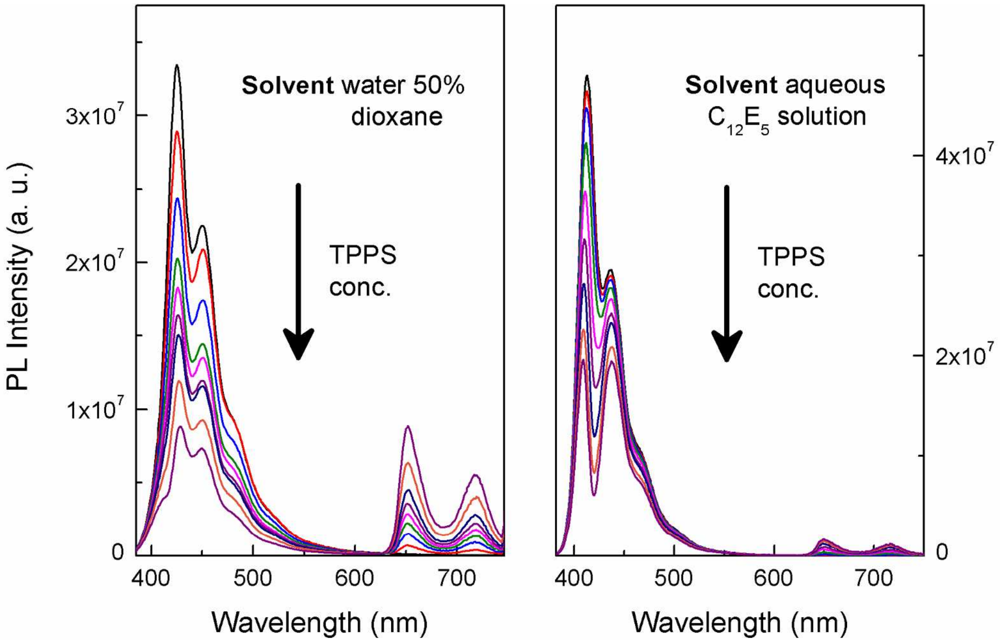

177x113mm (300 x 300 DPI)

Energy Transfer from Fluorene Based Conjugated Polyelectrolytes to On-chain and Self-Assembled Porphyrin Units

Ana T. Marques [a,b], Sara M. A. Pinto [a], Carlos J. P. Monteiro [a], J. Sérgio Seixas de Melo [a], Hugh D. Burrows [a], Ullrich Scherf [b], Mário J. F. Calvete [a] and Mariette M. Pereira [a]

[a] *Chemistry Department, University of Coimbra, Rua Larga 3004-535, Coimbra, Portugal*

[b] *Makromolekulare Chemie, Bergische Universität Wuppertal, , D-42097 Wuppertal, Germany*

Abstract

A new water soluble fluorene based polyelectrolyte containing on-chain porphyrin units has been synthesised via Suzuki coupling, for use in optoelectronic devices. The material consist of a random copolymer of poly{1,4-phenylene-[9,9-bis(4-phenoxy butylsulfonate)]fluorene-2,7-diyl} (PBS-PFP) and a 5,15-diphenylporphyrin (DPP). The porphyrin concentration was kept low (around 10% molar) to prevent copolymer aggregation and its consequent fluorescent quenching. The energy transfer process between the PBS-PFP units and the porphyrin has been investigated through steady state and time resolved measurements. The copolymer PBS-PFP-DPP displays two different emissions one located in the blue region of the spectra, corresponding to the fluorene part and another in the red, due to fluorescent DPP units either formed directly or by exciton transfer. However, relatively inefficient energy transfer from the PFP to the on-chain porphyrin units was observed. We compare this with a system involving an anionic blue-light-emitting donor PBS-PFP and anionic red-light-emitting energy acceptor *meso*-tetrakisphenylporphyrinsulfonate (TPPS), self-assembled by electrostatic attraction induced by Ca^{2+}. Based on previous studies related to chain aggregation of the anionic copolymer PBS-PFP, two different solvent media were chosen to further explore the possibilities of the self-assembled system: dioxane-water co-solvent and the non-ionic surfactant n-dodecylpentaoxyethylene glycol ether ($C_{12}E_5$). In contrast, with the on-chain PBS-PFP-DPP system, the strong overlap of the 0-0 emission peak of the PBS-PFP

and the Soret absorption band of the TPPS results in an efficient Förster transfer (FRET). This is strongly dependent upon the solvent medium used.

Introduction

The development of efficient conjugated polymer materials for organic electronics is a challenging area, with intensive ongoing research in topics such as organic light emitting diodes (OLEDs), organic field effect transistors (OFETs), photovoltaics, sensors and nanowires [1-6]. The addition of different chromophores as functional units to these conjugated polymer (CP) systems allows the introduction of new properties by tuning the emission through electronic energy transfer, and hence, the design of new intelligent materials [4-9]. In OLEDs, full-colour displays can be achieved by combining blue light-emitting fluorescent materials (either as emitter or as hosts) with green and red fluorescent dopants as the emitters [10-14]. Initial studies on such energy transfer systems generally used blends of donor and acceptor. However, this has the limitation that it often leads to phase separation. Greater efficiency may be anticipated if the chromophore is attached to the conjugated polymer, either by covalently bonding in the backbone, or by linking to the side chains. When bonding is in the main chain, the electronic structure, HOMO/LUMO levels and bandgaps of CPs can be manipulated through arrangement of electron or energy donor (D) and acceptor (A) units [15-17]. Such covalent attachment of a dye molecule to the polymer backbone, will broaden the absorption window of the conjugated polymer, and extend it to longer wavelengths [18-20]. This is of particular importance in polymer bulk heterojunction (BHJ) solar cell devices, since extending the spectral range of the polymeric material to the red region will increase light absorption by the active layer, leading to higher short-circuit currents and efficiencies [18-22]. In contrast to these structural and spectral advantages, experimental studies indicate that intra-chain energy transfer in isolated polymer chains is up to an order of magnitude less efficient than energy transfer between chains in polymer films. [23] Our goal is to develop methods of increasing electronic energy transfer within isolated conjugated polymer chains.

Poly(*para*-phenylene) type polymers (PPP) and the related polyfluorenes (PFs) are a particularly interesting class of conjugated polymers. PFs display high photoluminescence efficiencies and quantum yield, both in solution and in solid state, with emission wavelengths in the blue spectral region, in addition to good thermal and photostablility [24, 25]. Fluorene based copolymers are also attractive as energy donors in Förster resonance energy transfer [26, 27] (FRET). By doping, or covalent attachment of a lower bandgap material in the PF main chain, the polymer emission can be tuned to longer wavelengths by FRET [28]. For red emission, either polar moieties, such as electron donor substituted pyran derivatives, or non polar ones involving extensive π conjugation, such as perylene derivatives or porphyrin-type macrocyclic compounds have been studied [29, 30]. Systems involving PFs and red emitting porphyrins are particularly good candidates for FRET because of the excellent spectral overlap of donor emission and acceptor absorption as is the case of systems involving PFs and porphyrins [30–35]. Porphyrins are compounds of interest because their valuable photophysical properties [36] allow their use in a large number of practical applications, such as molecular photonic devices, artificial photosynthetic systems and dye-sensitized solar cells [4, 18, 37-39]. Also, porphyrins bearing hydrophilic pendant groups are able to interact with relevant biomolecules, as nucleic acids, polypeptides and proteins [40]. In addition, these are excellent systems for testing models of electronic energy transfer in conjugated polymers [41 - 44]. In particular, the Förster model for electronic energy transfer using point dipoles appears to break down at small PF-porphyrin distances, and the efficiency of energy transfer is suggested to show considerable differences if the two moieties are colinear or cofacial [43]. In this paper we compare singlet-singlet electronic energy transfer in two fluorene based anionic conjugated polyelectrolytes which have different PF-porphyrin orientations. For the colinear system, we synthesized an anionic poly(fluorene-*alt*-phenylene) with porphyrin units incorporated randomly on the backbone (Scheme 1). In the second system, we have self-assembled the polymer and porphyrin. We have previously shown electronic energy transfer within a self-assembled system involving anionic porphyrins and cationic fluorene based conjugated polyelectrolytes [32]. Metal ions, such as calcium(II), can also induce self-assembly of anionic conjugated polyelectrolytes [45, 46]. We extend this to calcium(II) induced self-assembly of an anionic poly(fluorene-*alt*-phenylene) conjugated polyelectrolyte and an anionic tetraphenylporphyrin, and have studied the electronic energy transfer both in large aggregates and surfactant modulated systems as models for cofacial energy transfer.

Experimental Section

Synthesis 2,7-dibromo-9,9-bis(4-sulfonylbutoxyphenyl)fluorene and poly{1,4-phenylene-[9,9-bis(4-phenoxy butylsulfonate)]fluorene-2,7-diyl} (**PBS-PFP**) were prepared according to published procedures and have been described elsewhere [41]. The synthesis of dipyrromethane and 5,15-diphenylporphyrin was carried out with slight modifications of previously described methods [47,48] see SI for the compounds characterization.

5,15-Dibromo-10,20-diphenylporphyrin, DPP. 300 mg of 5,15-diphenylporphyrin (0.58 mmol) were dissolved in 300 mL $CHCl_3$ and 2.4 mL of pyridine. The mixture was cooled to 0°C and 240 mg of *N*-bromosuccinimide (1.22 mmol, 2.1 eq) were added and the solution was stirred for 60 min. The reaction was quenched with acetone (50 mL) and the solvent was evaporated yielding a product that was washed with methanol [48]. Recrystallization from toluene/MeOH gave 347 mg of the title compound as purple crystals (0.56 mmol, 96%) ^{1}H NMR (400 MHz, $CDCl_3$) 9.62 (d, *J* = 4.7 Hz, 4H, H_β), 8.84 (d, *J* = 4.7 Hz, 4H, H_β), 8.17-8.15 (m, 4H, Ph-H*o*), 7.83-7.75 (m, 6H, Ph-H*m,p*), -2.72 (br s, 2H, NH).

The HOMO values of the DPP were measured using atmospheric pressure photoelectron spectrometry (Riken *Keiki AC-2*) and the LUMO calculated from the HOMO and optical band-gap (determined via the intersection of the absorption and emission thin film spectra) [49-51]. HOMO = 5.04 eV and LUMO = 3.17 eV.

Poly{1,4-phenylene}-*co*-{[9,9-bis(4-phenoxy butylsulfonate)]fluorene-2,7-diyl}-*alt*-{1,4-phenylene(5,15-diphenylporphyrin) PBS-PFP-DPP. For the preparation of the copolymer PBS-PFP-DPP, a mixture of 2,7-dibromo-9,9-bis(4-sulfonylbutoxyphenyl)fluorene (0.742 g, 0.90 mmol), 5,15-dibromo-10,20-diphenylporphyrin, DPP (0.062 g, 0.10 mmol), 1,4-benzenediboronic acid (0.166 g, 1 mmol), $Pd(PPh_3)_4$ (50 mg) and Na_2CO_3 (1.0 g, 9.4 mmol) [41] in 40 mL of THF and 20 mL water, were reacted for 4 days at 110 °C. The aqueous layer was washed with chloroform and concentrated to dryness. The residue was extracted with dichloromethane *via* Soxhlet, redissolved in a mixture of water and THF 50% (v/v) and purified by dialysis using a membrane with a cut-off of 3500 g·mol^{-1}. Based on the monomer/DPP ratio in the starting reaction mixture, the copolymer is expected to contain on average 10% (mole percent) DPP units. Total yield of the copolymer PBS-PFP-DPP was 655mg (91%). ^{1}NMR (600 MHz, d-THF 50% D_2O, ppm) 8.95-8.87 (ar-H DPP), 8.2 – 6.6 (ar-H DPP and ar-H fluorene), 4.1-3.9 (γ -CH_2), 2.98-2.86 (α -CH_2), 2.0-1.9 (β, δ -CH_2).

GPC (NMP, LiBr, UV-detection) M_w = 1400 g.mol^{-1}, M_w/M_n = 1.4. The M_w of the copolymer are likely to be considerably underestimated due to the interactions between the polyelectrolytes and the column material.

Steady State Spectroscopic Measurements. The measurements were recorded in water, and dioxane - water (1:1). All the solvents were of spectroscopic grade and Milli-Q water was used. To ensure almost complete dissolution of the copolymer, solutions were stirred overnight. Non-ionic surfactant n-dodecylpentaoxyethylene glycol ether ($C_{12}E_5$) was purchased from Aldrich and used without further purification. Absorption spectra were recorded using a Shimadzu UV-2100 spectrophotometer with a minimum resolution of 0.2 nm. For the steady-state measurements, fluorescence spectra were recorded with a Horiba-Jobin-Ivon SPEX Fluorog 3-22 spectrometer and were corrected for the instrumental response of the system. Fluorescence quantum yields were measured using quinine sulfate in 0.5 M sulfuric acid (for the poly(fluorene-*alt*-phenylene) region) and *meso*-tetrakis-phenylporphyrin (TPP) in toluene (for the DPP region) as references. Corrections were made for changes in refractive index [52].

Picosecond TCSPC Experiments. Picosecond time-resolved fluorescence measurements were performed using a home-built picosecond TCSPC apparatus, in which the excitation source consists of a picosecond Spectra Physics mode-lock Tsunami laser (Ti : sapphire) model 3950 (repetition rate of about 82 MHz, tuning range 700-1000 nm), pumped by a Millennia Pro-10s, frequency-doubled continuous wave (CW), diode-pumped, solid-state laser (λ_{em}=532 nm). A harmonic generator model GWU-23PS (Spectra-Physics) is used to produce the second and third harmonic from the Ti : sapphire laser exciting beam frequency output. The samples were measured with excitation at 372 nm and the horizontally polarized output beam from the GWU (second harmonic) was first passed through a ThorLabs depolarizer (WDPOL-A) and after by a Glan-Thompson polarizer (Newport 10GT04) with vertical polarization. Emission at 90° geometry collected at magic angle polarization was detected through a double subtractive Oriel Cornerstone 260 monochromator by a Hamamatsu microchannel plate photomultiplier (R3809U-50). Signal acquisition and data processing was performed employing a Becker & Hickl SPC-630 TCSPC module. Fluorescence decays and the instrumental response function (IRF) where collected using 4096 channels in a 0.814, 6.1 and 9.8 ps/channel scale, until 1.5×10^3 and 3×10^3 counts at maximum were reached. The full width at half-maximum (fwhw) of the IRF was about 22 ps and was highly reproducible with identical system parameters. A more detailed description of this equipment can be found in ref. 53.

Results and Discussion

Absorption and Fluorescence

The anionic copolymer poly(fluorene-*alt*-phenylene)-porphyrin (PBS-PFP-DPP) (Scheme 1) was studied by UV-Vis absorption, photoluminescence (PL) spectroscopy and time-resolved fluorescence (TS-SPC) measurements. Anionic fluorene based conjugated polyelectrolytes tend to aggregate in aqueous solution to form ill defined clusters. [54] To minimize this, measurements have been made in a 1:1 dioxane-water mixture and in water in the presence of $1x10^{-4}$ M non-ionic surfactant $C_{12}E_5$.

Scheme 1. Chemical structures of the homopolymer PBS-PFP, the DPP monomer and the copolymer PBS-PFP-DPP.

In both solvent systems two characteristic absorption regions are observed in the UV-Vis absorption spectrum, which are attributed to the poly(fluorene-*alt*-phenylene) backbone (broad absorption at 365 nm) and to the on-chain porphyrin (DPP) units (various bands between 420 and 650 nm) – Table 1, Figures 1 and 2. The strong narrow absorption peak at 420 nm and the four smaller absorption peaks between 520 and 650 nm correspond to the so-called “Soret” and “Q” bands, respectively, typical of porphyrins. [55] The presence of four absorptions in the Q band region, corresponding to the (0,0) and (0,1) vibronics of the Qx and Qy bands, confirms that the porphyrin is present as its free base. Excitation of PBS-PFP-DPP at 365 nm leads to emission from both PF and DPP, while excitation at 420 nm shows only emission from the DPP units (Figures 1 and 2). Fluorescence excitation spectra for emission in the porphyrin region reveals two maxima in the PF and DPP region, demonstrating efficient electronic energy transfer from the fluorene to the porphyrin units. However, differences in the relative intensities are observed in dioxane-water and in 1×10^{-4} M aqueous $C_{12}E_5$ solutions. In particular, the ratio of PF to DPP intensities is higher in $C_{12}E_5$ solution than in dioxane-water. Small angle X-ray scattering (SAXS), cryotransmission electron microscopy, molecular dynamics simulations, [56] together with small angle neutron (SANS) scattering on PBS-PFP solutions in the presence of $C_{12}E_5$ [57], strongly suggest that in the presence of $C_{12}E_5$, the conjugated polymer is present as a mixed cylindrical aggregate in which the polymer backbone is surrounded by a layer of surfactant molecules. Furthermore, a similar effect was observed with the closely related poly{9,9-bis[6-(N,N,N-trimethylammonium)alkyl]fluorene-co-1,4-phenylene} iodide cationic conjugated polyelectrolyte [58]. This is expected to have the two effects of increasing backbone rigidity and at the same time decreasing solvent access to the PF chain. We believe that with PBS-PFP-DPP, the increased rigidity will facilitate on-chain exciton migration and, hence, the efficiency of energy transfer to the porphyrin unit.

Quantum efficiency (PLQY) measurements made for the PBS-PFP-DPP copolymer in the solvent mixture dioxane-water (1:1) and in an aqueous solution of non-ionic surfactant $C_{12}E_5$ are presented in Table 1. The energy transfer quantum yields for PFP to DP units in greater in $C_{12}E_5$ solution than in 1/1 dioxane water. This may be associated with decrease in conformational disorder when encapsulated by the surfactant and is consistent with the results from the fluorene excitation spectra. There is a slight decrease in the PLQY values for the copolymer PBS-PFP-DPP compared with that of the polymer without the porphyrin chromophore, PBS-PFP, for the same solvents, 0.52 in water dioxane (1:1) and 0.45 [59] in $C_{12}E_5$. In part, this may result from photogenerated excitons being transferred to the DPP units. However, the sum of PLQY for emission from PF and DPP units is, in both cases, less than with PBS-PFP in the two solvents, indicating that some loss mechanism is also involved.

As shown in Figure 3, there is a strong overlap between the 0–0 emission band of the homopolymer PBS-PFP and the Soret absorption of the DPP; since the emission from the Soret band is weak, it acts as a dark state and the emission arises preferentially from the lowest energy Q_x band [35].

Table 1. Photophysical parameters of PBS-PFP-DPP in dioxane-water (1:1) and 1×10^{-4} M $C_{12}E_5$.

Figure 1. a) Absorption (solid line) and emission spectra (dashed line) of PBS-PFP-DPP in dioxane-water (1:1), with excitation at 365 nm (dashed line) and 420 nm (dotted line). The inset depicts the 600 – 750 nm region of the PBS-PFP-DPP emission shown in the main plot. **b)** Fluorescence excitation spectra with emission at 410 nm (solid line) and emission at 655 nm (dashed line) of PBS-PFP-DPP in dioxane-water (1:1).

Figure 2. a) Absorption (solid line) and emission spectra (dashed line) of PBS-PFP-DPP in 1×10^{-4} M aqueous $C_{12}E_5$ solution, with excitation at 365 nm (solid line) and 420 nm (dotted line). **b)** Fluorescence excitation spectra with emission at 410 nm (solid line) and emission at 655 nm (dashed line) of PBS-PFP-DPP in 1×10^{-4} M aqueous $C_{12}E_5$.

Figure 3. Spectral overlap between the donor PBS-PFP (dotted line) and the acceptor DPP (full line).

Time-resolved fluorescence

Fluorescence decays were obtained in the dioxane-water (1:1) mixture upon excitation in the poly(fluorene-*alt*-phenylene) unit (372 nm) and collecting at the PF and DPP emission maximum (Figure 4 and Table 2). A value of 550 ps (τ_3) that dominates the decay, together with a shorter lifetime value of 60 ps (τ_1) is found when the data is collected at 410 nm in agreement with previous observations [60]. The longer decay lifetime (τ_3) has a value very close to the previously described for PBS-PFP dispersed in the $C_{12}E_5$ micellar system [41, 61] and is attributed to the natural decay of the PF backbone [41]. The fast component (τ_1) is suggested to be related either to the formation of an initially formed non-relaxed conformer that decays giving rise to a more stable one [60], or to on-chain energy transfer process [60]. Nevertheless, sums of three discrete exponentials functions were needed to fit the excited state data collected at 650 nm. In dioxane-water, an intermediate decay component of 130 ps is observed. A similar decay time of approximately 130 ps has been reported previously for the cluster morphology adopted by polyelectrolytes in solution [62]. However, this seems unlikely in the present case, and, in agreement with suggestions of a closely related self assembled porphyrin/conjugated polyelectrolyte system we feel that this component is more likely due to exciton migration along the polymer chain [32]. This component becomes longer lived and more important in $C_{12}E_5$ solutions, the system showing more efficient energy migration from PF to DPP units. The 4.87 ns component is assigned to emission from the DPP units, in agreement with the values published for PPV and PF doped with porphyrins [34, 63].

Table 2. Fluorescence decay times (τ_i) and pre-exponential factors (a_{ij}) for the copolymer PBS-PFP-DPP, obtained with excitation at 372 nm, emission (λ_{em}) at the wavelength maxima and T= 298 K.

Figure 4. Fluorescence emission decay for PBS-PFP-DPP in dioxane water (1:1) collected at **a)** 410 nm and **b)** 650 nm obtained with λ_{exc} 372 nm at 298.15 K. The gray lines in the decays are the instrumental response function (IRF). For a better judgment of the quality of the fits, weighted residuals (W.R. scale, $-3 \leq \sigma \leq +3$), autocorrelation functions (A.C.) and χ^2 are also presented.

TPPS self-assembled with PBS-PFP via calcium (II) binding

With PBS-PFP-DPP, the porphyrin is expected to be collinear with the PF units. We will now discuss the second PF-porphyrin energy transfer system in which the anionic porphyrin TPPS is self-assembled by calcium(II) ions to the homopolymer PBS-PFP (Scheme 2), and the PF and porphyrin units are expected to be cofacial. The potential application of this system in sensing and in molecular logic will be described elsewhere. [64] We have previously reported the photophysics of a cationic PFP system self assembled by electrostatic interactions to TPPS. [32] These self-assembled systems have the advantage that by tuning the solvent and stoichiometry, it is possible to control the amount of porphyrin and, possibly, structural morphology and disorder of the materials. The characterization of the hydrophilic porphyrin has been described elsewhere. [65] The absorption and emission spectra of PBS-PFP were recorded in the same solvents used with PBS-PFP-DPP, dioxane-water (1:1) and $1x10^{-4}$ M aqueous $C_{12}E_5$ solutions (above the surfactant critical micelle concentration, cmc).

Scheme 2. Structure of the electronic energy acceptor *meso*-tetrakisphenylporphyrinsulfonate, TPPS.

Calcium (II) modulates the self-assembly between the two negatively charged components. Energy transfer from the PBS-PFP to the anionic porphyrin is evident from the PL spectra (Figure 5). By adding different concentrations of porphyrin to the polyelectrolyte at fixed Ca^{2+} concentration 2×10^{-3} M there was a decrease in the fluorescence band in the PF region and a corresponding increase seen in the emission band of the porphyrin (λ_{max} = 650 nm). The quenching effect is most pronounced when the polyelectrolyte is dissolved in the dioxane-water co-solvent solution mixture, see Figure 6. As will be seen, significant differences are seen in energy transfer from PF to porphyrin units in the on-chain and self-assembled systems, in agreement with the predictions of Wong et al. [42] In addition to effects of orientation of the donor-acceptor units, other non-radiative deactivation processes may be possible in the PBS-PFP-DPP copolymer, including charge transfer, triplet formation, exciton – exciton annihilation and molecular excimer formation [35, 66, 67]. With the low light intensity and dilute solutions used, the latter two processes are unlikely.

For the self-assembled system, control experiments of the effect of $2x10^{-3}$ M Ca^{2+} on the photoluminescence of the PBS-PFP copolymer solutions were also performed and no significant differences were observed in the spectral shape or maximum (see SI). Nevertheless, the PLQY decreases in the presence of Ca^{2+} as a consequence of the metal interaction with the polar copolymer side chains inducing aggregation. [46] The photoluminescence deactivation by Ca^{2+} of the copolymer in the 1:1 dioxane-water mixture is 30% more effective than in the surfactant solution (see SI). The spectral changes observed in the PL spectra (Figure 7) are mainly due to the strong attenuation by the overlap of the absorption of the porphyrin Soret band and the PBS-PFP copolymer fluorescence (Figure 3) [32]. The PL quenching is more pronounced in dioxane-water (1:1) mixture, Figure 5 and Table 3, since calcium ion induces strong copolymer-aggregation [46], and the large aggregates are likely to favour energy transfer from multiple PBS-PFP units towards TPPS. In contrast, for the self-assembled system in the presence of the non-ionic surfactant, a lower PLQY was found for the TPPS on excitation of PBS-PFP (Table 3). It is known that $C_{12}E_5$ wraps around the copolymer forming supramolecular structures that shield the PBS-PFP from the aqueous solvent. [55, 68] This means that calcium ions are likely to only bind to the exposed sulfonate groups on a single PBS-PFP chain, such that energy transfer is from one CPE molecule to the bound porphyrin. Small angle X-ray (SAXS) and neutron (SANS) scattering studies are in progress to obtain more structural information on these systems.

Figure 5. Photoluminescence spectra of PBS-PFP/Ca^{2+} with increasing TPPS concentrations in water dioxane (1:1) (**left**) and in 1×10^{-4}M $C_{12}E_5$ (**right**). Ca^{2+} concentration $2x10^{-3}$ M.

Figure 6. Photoluminescence maximum intensity as a function of TPPS concentration in water dioxane (1:1) (**left**) and in 1×10^{-4}M $C_{12}E_5$ (**right**); **squares**: PBS-PFP emission and **triangles**: TPPS emission.

Figure 7. Photoluminescence spectra of PBS-PFP without TPPS (**solid line**) and with maxima TPPS concentration (**dot line**), obtained with excitation in the PF

absorption maximum and TPPS emission (**dash line**) obtained with excitation at 420 nm, in water dioxane (1:1) (**right**) and in 1×10^{-4}M $C_{12}E_5$ (**left**).

Table 3. Photoluminescence quantum yields of PBS-PFP/Ca^{2+} self assembled with TPPS in dioxane water (1:1) and 1×10^{-4} M $C_{12}E_5$ (Ca^{2+} concentration $2x10^{-3}$ M).

Fluorescence decays of the system PBS-PFP+Ca^{2+}+TPPS, with increasing anionic porphyrin concentration were collected at the PBS-PFP. The decays were fitted with sums of three discrete exponential functions and the corresponding decay times and amplitudes, as a function of the porphyrin concentration, are plotted, Figure 8.

Figure 8. Fluorescence decay times (τ_i) and amplitudes (a_{ij}) of PBS-PFP (10^{-6} M) with Ca^{2+} (1×10^{-3} M) in 1×10^{-4} M $C_{12}E_5$ as a function of TPPS concentration.

Figure 9. Fluorescence emission decay of PBS-PFP (10^{-6} M) with Ca^{2+} (1×10^{-3} M) in 1×10^{-4} M $C_{12}E_5$ and TPPS concentration maxima, obtained with λ_{exc} 392 nm at 298.15 K. The gray lines in the decays are the instrumental response function (IRF). For a better judgment of the quality of the fits weighted residuals (W.R. scale, $-3 \leq \sigma \leq +3$), autocorrelation functions (A.C.) and χ^2 are also presented.

The dependence of the decay times and amplitudes, presented in Figure 8 is similar to the behaviour observed for the system involving the cationic fluorene based polyelectrolyte HTMA-PFP and different hydrophilic porphyrins [32]. The long component (τ_3) has a value very close to that previously reported for PBS-PFP with $C_{12}E_5$ in water [41] and the presence of calcium does not seem to affect the lifetime of the polyelectrolyte, see SI. The PBS-PFP lifetime is, as previously observed in the PL data, quenched with increasing porphyrin concentration

(Figure 6). Attribution of the fastest component (τ_1 ca. 20 ps for a TPPS concentration of 8.03×10^{-7} M) is still troublesome and it has been attributed to both energy transfer and conformational relaxation of the copolymer chain [32, 60]. However, with the present system and based on the decay profile and data of Figure 9, a rise time (ca. 7 ps at the same TPPS concentration) is attributed to the fast component, providing evidence that energy transfer is taking place and dominating the deactivation pathways occurring in the excited states of the self-assembled donor/acceptor system. The origin of the intermediate lifetime component, τ_2, has been discussed previously and attributed to exciton migration, either on-chain or intra-chain (within aggregates) [32, 62].

The PL efficiency of the self-assembled system is always greater than with the copolymer PBS-PFP-DPP. This resembles the behaviour described for MEH-PPV porphyrin blends [69]. As demonstrated by Morgado *et al.* the distribution of the porphyrin chromophore within the polymer does not match the one for the self-assembled system and the copolymer. Hence, the differences in the efficiency of the energy transfer and the concentration quenching effects might contribute for the different observations. The results are also in complete agreement with the ideas of Wong et al. on cofacial energy transfer in PF-porphyrin systems being more efficient than the collinear case. [42] Whilst the porphyrin ring and polymer backbone may not be perfectly parallel, a small deviation from cofacial geometry is not likely to significantly affect the efficiency of Förster energy transfer. Although these authors have questioned the validity of the use of point dipoles in Förster theory [70, 71] to treat electronic energy transfer between these donor and an acceptor units, it is instructive to compute the radius, R_0 that identify the distance at which the transfer occurs with 50% efficiency. Table 4 comprise the R_0 values for the PBS-PFP-DPP copolymer and for the self-assembled system PBS-PFP/TPPS.

Table 4. Föster radius, R_0, of PBS-PFP-DPP and of PBS-PFP with TPPS.

As expected the R_0 value vary for the two systems according to PBS-PFP/TPPS ≤ PBS-PFP-DPP. However, the efficiency of the porphyrin PL runs counter to expectation on the basis of Förster theory, since the copolymer PBS-PFP-DPP is the least efficient despite the larger R_0 value [72]. As mentioned before, when we discussed the properties of the PBS-PFP-DPP, were discussed other factors than the Förster efficiency govern the copolymer PL efficiency [72]. Overall the values calculated for the Förster distance are comparable to what had been determined for the singlet-singlet Förster transfer, from fluorene-based polyelectrolytes and oppositely charged complexes and porphyrins [32, 73].

Conclusions

We have explored the mechanisms for energy transfer in two fluorene based conjugated polyelectrolytes (donor) systems, with on-chain porphyrin moieties and self-assembled with an anionic porphyrin bound electrostatically by Ca^{2+}.

Investigation of the photophysical properties of the CPEs leads to the conclusion that the polymers are relatively free from aggregation in the solvent mixtures, $C_{12}E_5$ and water organic co-solvent.

Time-resolved experiments and steady state measurements have been conducted in solution to unravel the role of energy transfer on both systems. The energy transfer process in the PBS-PFP-DPP case should compete with other deactivaction processes, such as radiative decay of the singlet excitons photogenerated on the donor-acceptor conjugated chains and copolymer solution conformational changes. The existing difference between the overall energy transfer efficiency among the PBS-PFP-DPP copolymer and the self-assembled system is attributed to the porphyrin chromophore content within the polymer, that is not necessarily equal to the TPPS solution concentration. As observed by Morgado and co-workers [69] the energy transfer efficiency values in a MEH-PPV porphyrin blend and in a MEH-PPV-porphyrin copolymer are similar only when the copolymer possesses the highest porphyrin concentration. Furthermore, the spatial extent, intermolecular separation and relative orientations of transition dipole densities on the donor and acceptor PF-porphyrin copolymers determinate the rate of electronic excitation transfer, as observed for the cofacial and collinear orientations between the donor and the acceptor.

Acknowlegments

Financial support from FCT (Fundação para a Ciência e a Tecnologia) is acknowledge through the attribution of the Ph.D grants of ATM (SFRH/BD/36666/2007), SMAP (SFRH/BD/47022/2008) and CJPM (SFRH/BD/37652/2007). Dr. João Pina from the University of Coimbra is acknowledged for his excellent technical support in the TCSPC experiments. We thank the Evonik Science to Business Center, Marl Germany, for the photoelectron spectroscopy measurements.

Bibliography

(1) Moons, E.; J. Phys.: Condens. Matter, **2002**, 14, 12235–12260.

(2) Hains, A. W.; Liang, Z.; Woodhouse, M. A.; Gregg, B. A.; Chem. Rev., **2010**, 110, 6689–6735.

(3) Wen, Y.; Liu, Y.; Adv. Mater., **2010**, 22, 1331–1345.

(4) Zöllner, M. J.; Frähmcke, J. S.; Elstner, M.; Jahn, U.; Jones, P. G.; Becker, E.; Kowalsky, W.; Johannes, H.-H.; Macromol. Chem. Phys., **2010**, 211, 359–371.

(5) Zou, Y.; Najari, A.; Berrouard, P.; Beaupré, S.; Aïch, B. R.; Tao, Y.; Leclerc, M.; J. Am. Chem. Soc., **2010**, 132, 5330–5331.

(6) Lei, T.; Cao, Y.; Fan, Y.; Liu, C.-J.; Yuan, S.-C.; Pei, J.; J. Am. Chem. Soc., **2011**, 133, 6099–6101.

(7) Huang, F.; Zhang, Y.; Liu, M. S.; Jen, A. K.-Y.; Adv. Funct. Mater., **2009**, 19, 1–10.

(8) Perzon, E.; Zhang, F.; Andersson, M.; Mammo, W.; Inganäs, O.; Andersson,

M. R.; Adv. Mater., **2007**, 19, 3308–3311.

(9) Berton, N.; Lemasson, F.; Tittmann, J.; Stürzl, N.; Hennrich, F.; Kappes, M. M.; Mayor, M.; Chem. Mater., **2011**, 23, 2237-2249.

(10) Wang, X.; Wang, H.; Yang, Y.; He, Y.; Zhang, L.; Li, Y.; Li, X.; Macromolecules, **2010**, 43, 709–715.

(11) Huang, X.; Shi, Q.; Chen, W.-Q.; Zhu, C.; Zhou, W.; Zhao, Z.; Duan, X.-M.; Zhan, X.; Macromolecules, **2010**, 43, 9620–9626.

(12) Ego, C.; Marsitzky, D.; Becker, S.; Zhang, J.; Grimsdale, A. C.; Müllen, K.; MacKenzie, J. D.; Silva, C.; Friend, R. H.; J. Am. Chem. Soc., **2003**, 125, 437–443.

(13) Huang, J.; Li, G.; Wu, E.; Xu, Q.; Yang, Y.; Adv. Mater., **2006**, 18, 114–117.

(14) Xu, Y.; Guan, R.; Jiang, J.; Yang, W.; Zhen, H.; Peng, J.; Cao, Y.; Journal of Polymer Science: Part A: Polymer Chemistry, **2008**, 46, 453–463.

(15) Meng, G.; Velayudham, S.; Smith, A.; Luck, R.; Liu, H.; Macromolecules **2009**, 42, 1995-2001.

(16) McNeill, C. R.; Greenham, N. C.; Adv. Mater., **2009**, 21, 3840–3850.

(17) Wu, P.-T.; Bull, T.; Kim, F. S.; Luscombe, C. K.; Jenekhe, S. A.; Macromolecules, **2009**, 42, 671–681.

(18) Campo, B. J.; Duchateau, J.; Ganivet, C. R.; Ballesteros, B.; Gilot, J.; Wienk, M. M.; Oosterbaan, W. D.; Lutsen, L.; Cleij, T. J.; de la Torre, G.; Janssen, R. A. J.; Vanderzande. D.; Torres, T.; Dalton Trans., **2011**, 40, 3979 – 3988.

(19) Kraft, A.; Grimsdale, A. C.; Holmes, A. B.; Angew. Chem. Int. Ed. , **1998**, 37, 402–428.

(20) Perepichka, I. F.; Perepichka, D. F.; Meng, H.; Wudl, F.; Adv. Mater., **2005**, 17, 2281–2305.

(21) Nunzi, J.-M.; C. R. Physique, **2002**, 3, 523–542.

(22) Dennler, G.; Scharber, M. C.; Brabec, C. J.; Adv. Mater., **2009**, 21, 1–16.

(23) Beljonne, D.; Pourtois, G.; Silva, C.; Hennebicq, E.; Herz, L. M.; Friend, R. H.; Scholes, G. D.; Setayesh, S.; Müllen, K.; Brédas, J. L.; PNAS, **2002**, 99, 10982 – 10987.

(24) Scherf, U.; List, E. J. W.; Adv. Mater., **2002**, 14, 477–487.

(25) Grimsdale, A. C.; Müllen, K.; Adv. Polym. Sci., **2008**, 212, 1 – 48.

(26) Schwartz, B. J.; Annu. Rev. Phys. Chem., **2003**, 54, 141–172.

(27) Abbel, R.; Grenier, C.; Pouderoijen, M. J.; Stouwdam, J. W.; Leclère, P. E. L. G.; Sijbesma, R. P.; Meijer, E. W.; Schenning, A. P. H. J.; J. Am. Chem. Soc., **2009**, 131, 833–843.

(28) Wu, C.; Zheng, Y.; Szymanski, C.; McNeill, J.; J. Phys. Chem. C**, 2008**, 112, 1772–1781.

(29) Li, C.; Bo, Z.; Polymer, **2010**, 51, 4273-4294.

(30) Dutta, P.; Rai, R.; Pandey S.; J. Phys. Chem. B, **2011**, 115, 3578–3587.

(31) Li, B.; Xu, X.; Sun, M.; Fu, Y.; Yu, G.; Liu, Y.; Bo, Z.; Macromolecules, **2006**, 39, 456-461.

(32) Pinto, S. M.; Burrows, H. D.; Pereira, M. M.; Fonseca, S. M.; Dias, F. B.; Mallavia, R.; Tapia, M. J.; J. Phys. Chem. B, **2009**, 113, 16093–16100.

(33) Wang, X.; Wang, H.; Yang, Y.; He, Y.; Zhang, L.; Li, Y.; Li, X.; Macromolecules **2010**, 43, 709–715.

(34) Lyons, B. P.; Jackson, R. J.; Wong, K. S.; Monkman, A. P.; Synthetic Metals, **2003**, 135 – 136, 367 – 368.

(35) Virgili, T.; Lidzey, D. G.; Bradley, D. D. C.; Synthetic Metals, **2000**, 111 – 112, 203 – 206.

(36) Song, J.; Aratani, N.; Kim, P.; Kim, D.; Shinokubo, H.; Osuka, A.; Angew. Chem. Int. Ed., **2010**, 49, 3617–3620.

(37) Kim, P.; Sung, J.; Uoyama, H.; Okujima, T.; Uno, H.; Kim, D.; J. Phys. Chem. B, **2011**, 115, 3784–3792.

(38) Yoneda, T.; Saito, S.; Yorimitsu, H.; Osuka, A.; Angew. Chem. Int. Ed., **2011**, 50, 3475–3478.

(39) Liddell, P. A.; Gervaldo, M. G.; Bridgewater, J. W.; Keirstead, A. E.; Lin, S.; Moore, T. A.; Moore, A. L.; Gust, D.; Chem. Mater., **2008**, 20, 135–142.

(40) Castriciano, M. A.; Romeo, A.; Angelini, N.; Micali, N.; Longo, A.; Mazzaglia, A.; Scolaro, L. M.; Macromolecules, **2006**, 39, 5489–5496.

(41) Burrows, H. D.; Lobo, V. M. M.: Pina, J.; Ramos, M. L.; de Melo, J. S.; Valente, A. J. M.; Tapia, M. J.; Pradhan, S.; Scherf, U.; Macromolecules, **2004**, 37, 7425–7427.

(42) Wong, K. F.; Bagchi, B.; Rossky, P. J.; J. Phys. Chem. A, **2004**, 108 5752 – 5763.

(43) Saini, S.; Srinivas, G.; Bagchi, B.; J. Phys. Chem. B, **2009**, 113, 1817 – 1832.

(44) Hwang, I.; Scholes, G. D.; Chem. Mater. **2011**, 23, 610 – 620.

(45) Jiang, H.; Zhao, X.; Schanze, K. S.; Langmuir, **2006**, 22, 5541 – 5543.

(46) da Costa, J. L. T.; Silva, C. L.; Valente, A. J. M.; Pais, A. A. C. C.; Burrows, H. D.; RICI-2 Colloids and Interfaces, SPQ, Coimbra, **2007**, p.533-537.

(47) Littler, B. J.; Miller, M. A.; Hung, C.-H.; Wagner, R. W.; O'Shea, D. F.; Boyle, P. D.; Lindsey, J. S.; J. Org. Chem., **1999**, 64, 1391–1396 .

(48) DiMagno, S. G.; Lin, V. S.-Y.; Therien, M. J.; J. Org. Chem., **1993**, 58, 5983–5993.

(49) Zhou, X.; Shen, P.; Zhao, B.; Jiang, P.; Deng, L.; Tan, S.; Journal of Polymer Science Part A: Pol. Chemistry, **2011**, 49, 2685–2692.

(50) Xu, X.; Chen, H.; Huo, E.; Cai, X.; Ying, Y.; Polymer Bulletin, 2008, 60, 7–14.

(51) Huang, X.; Zhu, C.; Zhang, S.; Li, W.; Guo, Y.; Zhan, X.; Liu, Y.; Bo, Z.; Macromolecules, 2008, 41, 6895–6902.

(52) Montalti, M.; Credi, A.; Prodi, L.; Gandolfi, M. T.; Handbook of Photochemistry, Taylor & Francis, **2006**.

(53) Pina, J.; Melo, J. Seixas de; Burrows, H. D.; Maçanita, A. L.; Galbrecht, F.; Bünnagel, T.; Scherf, U.; Macromolecules, **2009**, 42, 1710.

(54) Burrows, H. D.; Fonseca, S. M.; Silva, C. L.; Pais, A. A. C. C.; Tapia, M. J.; Pradhan, S.; Scherf, U.; Phys. Chem. Chem. Phys., **2008**, 10, 4420–4428.

(55) Gouterman, M.; J. Mol. Spectrosc., **1961**, 6, 138 – 163.

(56) Burrows, H. D.; Tapia, M. J.; Fonseca, S. M.; Pradhan, S.; Scherf, U.; Silva, C. L.; Pais, A. A. C. C.; Valente, A. J. M.; Schillén, K.; Alfredsson, V.; Carnerup, A. M.; Tomsic, M.; Jamnik, A.; Langmuir, **2009**, 25, 5545 – 5556.

(57) Knaapila, M.; Almásy, L.; Garamus, V. M.; Pradhan, S.; Pearson, C.; Petty, M. C.; Scherf, U.; Burrows, H. D.; Monkman, A. P.; J. Phys. Chem. B, **2006**, 110, 10248 – 10257.

(58) Burrows, H. D.; Knaapila, M.; Monkman, A. P.; Tapia, M. J.; Fonseca, S. M.; Ramos, M. L.; Pyckhout-Hintzen, W.; Pradhan, S.; Scherf, U.; J. Phys. Cond. Matter, **2008**, 20, 102410.

(59) Burrows, H. D.; Tapia, M. J.; Fonseca, S. M.; Valente, A. J. M.; Lobo, V. M. M.; Justino, L. L. G.; Qiu, S.; Pradhan, S.; Scherf, U.; Chattopadhyay, N.; Knaapila, M.; Garamus, V. M.; Appl. Mater. Interfaces, **2009**, 1, 864–874.

(60) Dias, F. B.; Maçanita, A. L.; de Melo, J. S.; Burrows, H. D.; Güntner, R.; Scherf, U.; Monkman, A. P.; J. Chem. Phys., **2003**, 118, 7119–7126.

(61) Burrows, H. D.; Fonseca, S. M.; Dias, F. B.; de Melo, J. S.; Monkman, A. P.; Scherf, U.; Pradhan, S.; Adv. Mater., **2009**, 21, 1155–1159.

(62) Al Attar, H. A.; Monkman, A. P.; Adv. Funct. Mater., **2008**, 18, 2498–2509.

(63) de Melo, J. S.; Sobral, A. J. F. N.; Gonsalves, A. M. d'A. R.; Burrows, H. D.; J. Photochem. Photobiol. A: Chemistry, **2005**, 172, 151–160.

(64) Burrows, H. D.; Calvete, M. J. F.; da Costa, J. L. T.; Fonseca, S. M.; Marques, A. T.; Monteiro, C. J. P.; Pereira, M. M.; Pinto, S. M. A.; Scherf, U.; Valente, A. J. M. manuscript in preparation.

(65) Monteiro, C. J. P.; Pereira, M. M.; Pinto, S. M. A.; Simões, A.V.C.; Sá, G. F. F.; Arnaut, L. G.; Formosinho, S. J.; Simões, S.; Wyatt, M. F., Tetrahedron, **2008**, 64, 5132–5138.

(66) Fujitsuka, M.; Okada, A.; Tojo, S.; Takei, F.; Onitsuka, K.; Takahashi, S.; Majima, T.; J. Phys. Chem. B, **2004**, 108, 11935–11941.

(67) Iqbal, R; Moratti, S. C.; Holmes, A. B.; Yahioglu, G.; Milgrom, L. F.; Cacialli, F.; Morgado, J.; Friend, R. H.; Journal of Materials Science: Materials in Electronics, **2000**, 11, 97–103.

(68) Tapia, M. J.; Monteserín, M.; Costoyas, A.; Burrows, H. D.; Marques, A. T.; Pais, A. A. C. C.; Valente, A. J. M.; Mallavia, R.; Scherf, U.; Pinazo, A.; Pérez, L.; Morán, M. C.; Journal of Molecular Liquids, **2010**, 156, 18–27.

(69) Morgado, J.; Cacialli, F.; Iqbal, R.; Moratti, S. C.; Holmes, A. B.; Yahioglu, G.; Milgrom, L. R.; Friend, R. H.; J. Mater. Chem., **2001**, 11, 278–283.

(70) Turro, N. J.; Modern Molecular Photochemistry, University Science Books **1991**.

(71) Lakowicz, J. R.; Principles of Fluorescence Spectroscopy, 3rd Edition, Springer **2006**.

(72) Tan, C.; Atas, E.; Müller, J. G.; Pinto, M. R.; Kleiman, V. D.; Schanze, K. S.; J. Am. Chem. Soc., **2004**, 126, 13685– 36949.

(73) Burrows, H. D.; Fonseca, S. M.; Dias, F. B.; de Melo, J. S.; Monkman, A. P.; Scherf, U.; Pradhan, S.; Adv. Mater., **2009**, 21, 1155–1159.